

Full Length Research Paper

Spatial distribution of rainfall seasonality over East Africa

Zablone Owiti^{1,2*} and Weijun Zhu¹

¹Key Laboratory of Meteorological Disaster, Nanjing University of Information, Science and Technology, Nanjing, China

²National Council for Science and Technology, Nairobi, Kenya

Accepted 16 April 2012

In this study, we have investigated the geographical variations of rainfall seasonality components over East Africa on the basis of pentad rainfall data at 36 stations during the period 1962-2006. Harmonic analysis was used to model the annual and semi-annual modes of rainfall seasonality at each station. The ratio of the modeled semi-annual range (R_2) to annual range (R_1) was used as an objective index to measure the degree of bimodal or unimodal behavior of rainfall at a given station. Areas of unimodal/bimodal regime were qualitatively delineated based on the difference of the fractional variance (V_1-V_2) explained by each of the modes. Results show that negative values of V_1-V_2 , signifying bimodal regime, compares well to R_2/R_1 exceeding 0.3. Stations in areas of transition between annual and semi-annual regimes have values of V_1-V_2 near zero indicating that neither of the two modes dominates. Results further show that the seasonality of rainfall over the whole region does not follow the classical scheme of north-south pattern with bimodal (unimodal) dominance in areas in the vicinity (north/south) of the equator. This scenario is only true for the western strip of the region between longitudes 29°E to 34°E.

Keywords: Rainfall, Seasonality, Annual, Semi-annual, East Africa

INTRODUCTION

This is a study of spatial characteristics of rainfall seasonality components over East African region (Figure 1). The East African region comprises of 3 countries: Kenya, Uganda and Tanzania. Major sectors of the region's economy like agriculture, heavily depend on the availability of water, and therefore, directly or indirectly on rainfall. The region experiences and is sensitive to large climate fluctuations in terms of floods and droughts which have resulted to disasters which the inhabitants have only marginally been able to cope with. In recent years, East Africa has suffered frequent episodes of both excessive (Webster et al. 1999; Latif et al. 1999) and deficient rainfall (Hastenrath et al. 2007) which impacted negatively on the economy. The severe drought over most

parts of the region in 2011 was one of the worst in the last 60 years. Another example is the extreme rainfall event of 1961 that led to disastrous floods in the region. Shongwe et al. (2011) showed that the frequency of disasters related to anomalously strong rainfall has increased over East Africa. This was based on their analysis of data from the International Disaster Database EM-DAT (<http://www.em-dat.net/>). Further analysis of twentieth and twenty first century simulations of African climate change with 19 models from the 3rd Coupled Model Intercomparison Project (CMIP3) archive by Giannini et al. (2008) show that majority of models agree on wetter conditions over eastern equatorial Africa.

Seasonal cycle is the largest climate signal; however its variability in space and time has been overlooked as a climate diagnostic. It is often removed (by considering anomalies from it) in studies concerning climate variability or change. However, previous studies, for example Pezzulli et al. (2005); Shen et al. (2005); and Wu et al. (2008) have shown that the seasonal cycle can contain

*Corresponding author: E-mail: zowiti@ncst.go.ke or zablonowiti@yahoo.com Tel: (+86) 18751909142. Fax (+86) 25 58699848

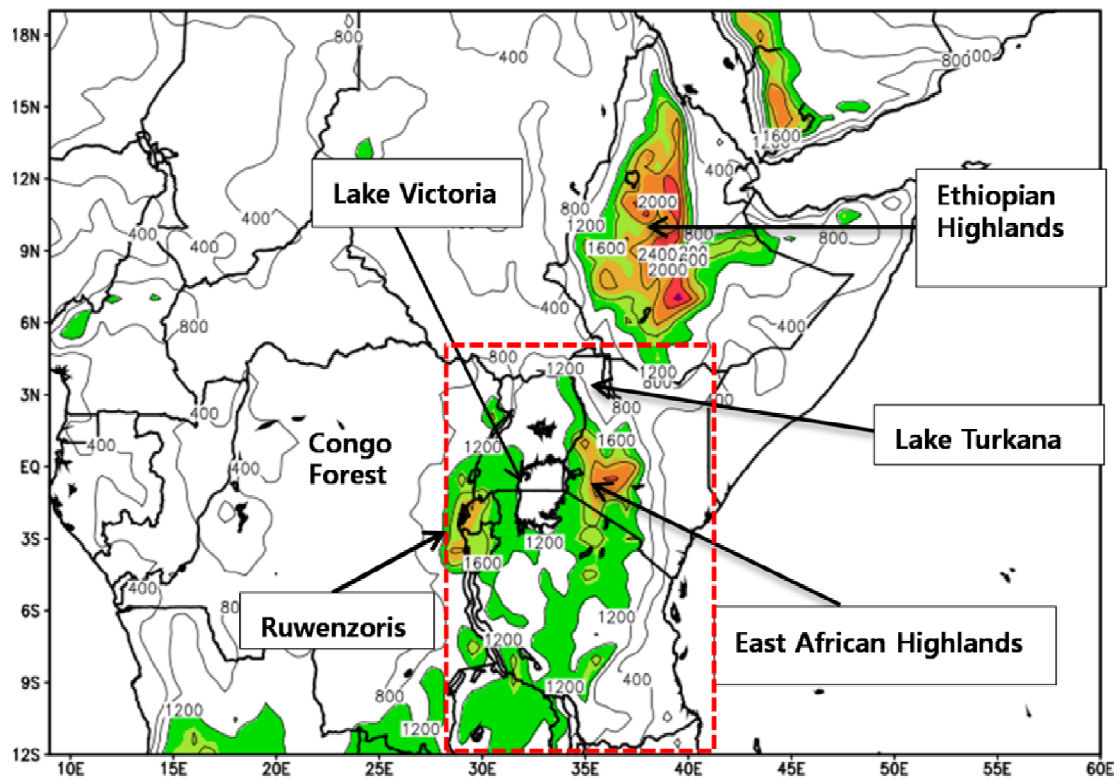


Figure 1: Topographical features of East Africa (EA) domain (*inner rectangle*), with areas higher than 1200m shaded.

amplitude-frequency modulation due to the nonlinearity of the climate system. Further, inter-annual variations in the seasonal cycle have been observed in climate time series (e.g. Thompson 1999; Bograd et al. 2002; and Whitfield et al. 2002) and deserve more careful attention. Knowledge of variability and change of seasonal cycle is therefore an important component in the understanding of climate variability. If various forcings of seasonal variability could be isolated, then it may be easier to understand the longer term variability such as inter-annual and decadal oscillations in a climate variable. Indeed, a description of the seasonal cycle of rainfall also allows for the dominant seasonal signal to be removed, to give a background for empirical analysis of longer time scale cycles fed by ocean-atmosphere dynamics to improve rainfall monitoring and prediction.

When evaluating the impact of rainfall on various sectors, its distribution throughout the seasonal cycle may be as important as the total annual rainfall. The interaction between the atmosphere's general circulation and major topographic features such as land masses, sea coasts, and mountain ranges produces seasonal distribution of rainfall. While previous studies (e.g. Nicholson 1996, Indeje et al, 2000) on East African rainfall climatology have provided a general understanding of the geographic patterns of seasonal distribution of rainfall, it is also important to define

accurately and quantify the boundaries of transition regions between areas of similar seasonality and also quantify the strength of annual and semi-annual seasonality components at specific sites/stations. This information can then be utilized in assessing changes in these boundaries and seasonality component strengths with time which could be either random or with changing climate. Moreover, the studies cited above used multi-stations averaged data to study the annual cycle evolution of rainfall and delineate the region into homogeneous zones. However, when data from several stations are combined, individual local peculiarities and errors arising from topography, the altitude, the exposure of the gauge and from other local controls are to a considerable degree smoothed out. In this part 1 of our study, we attempt to clarify using more quantitative technique, the seasonality pattern of rainfall across East African region with respect to the annual and semi-annual seasonality components by using the available gauge data to model the seasonality components at all locations and provide their spatial presentation. Part 2 of this study which is under preparation will assess if there have been any decadal changes in the seasonality components of rainfall over East Africa.

Different analytical approaches have been utilized to quantify and simplify the description of climate events. Principal Component (PC) analysis has been frequently

used in the analysis of rainfall patterns over African and other regions. For example, Mpeta and Jury (2005) used PC analysis to describe the attributes of the annual cycle of African climate and how it relates to climate variability. In this study Harmonic analysis is used to model the annual cycle based on the mean pentad gauge rainfall at each of 36 stations over the region to assess the relative strength of its annual and semi-annual components.

DATA AND METHOD

Two different regional precipitation data sets were used in this analysis. The first is based on the gauge station rainfall in 36 stations in the region that had station daily data for the period 1962 – 2006. The second data set is based on the spatially interpolated, gridded data set from the University of Delaware.

Gauge-observed rainfall data

Like the rest of Africa, East Africa continues to experience some difficulties with the availability of long-time climate data (Camberlin and Philippon, 2002). Furthermore, the available data are also riddled with numerous gaps in both space and time. These limitations in the quantity and quality of in situ observations impose substantial constraints on diagnostic studies of the regional climate (rainfall) variability. Available are sparse surface observations whose number has tremendously reduced over time. The observed daily rainfall amounts for 36 stations across the three East Africa countries (Kenya, Uganda and Tanzania), extending from January 1962 to December 2006 was used in this study. Table 1 provides details of stations used in terms of location and elevation.

University of Delaware Gridded Precipitation Data

The University of Delaware gridded monthly precipitation (V2.01) data set (Willmott and Matsuura, 2009) is provided by the NOAA/OAR/ESRL PSD, Boulder, Colorado, USA, from their Web site at <http://www.esrl.noaa.gov/psd/>. The data, gridded at 0.5 x 0.5 degree resolution spans from 1900 – 2008. The data has advantage of being available at higher resolution and longer period of time compared to other gridded data sets and is also easily available. Further the University of Delaware dataset benefits from the inclusion of Sharon Nicholson's African gauge data (Nicholson, 2001) for 1950-1996 (Parker et al., 2011). The dataset contains a large number of gauges that have not been included in other datasets. This data was used in this study to show the time-latitude cross-section of zonally averaged mean rainfall over delineated sub-regions based on the characteristics of the modeled annual cycle components to visualize their variability from a time-latitude perspective.

Method

Harmonic analysis was used to fit the annual and semi-annual components seasonality of rainfall series at each station. This method provides a convenient vector for displaying annual and semi-annual Fourier harmonics. A number of studies for example Hamada et al (2002) and Filkenstein and Truppi (1991) have used harmonic analysis to describe rainfall series by a series of harmonic terms. In this analysis it is assumed that rainfall over the region will either be unimodal (one maximum per year) or bimodal, requiring that only two harmonic terms be used. Thus the annual and

semiannual modes are the first two harmonics of the climatologically averaged annual rainfall variation at each location. Harmonic analysis consists of representing the fluctuations or variations of time series as having arisen from adding together of a series of a sine and cosine functions. These trigonometric functions are trigonometric in the sense that they are chosen to have frequencies exhibiting integer multiples of fundamental frequency determined by the sample size of the data series. In this study, the historical gauge pentad station rainfall data was subjected harmonic analysis to derive the amplitude (C_k) and phase (φ_k) of the annual and semi-annual rainfall cycle for the 36 stations that had daily rainfall data. This was done by dividing one analysis year into 73 pentads from 1st January to 31st December. Data on February 29 in a leap year was included into pentad 49 (February 25–March 1). The pentad-mean was averaged for the period 1971–2000 at each of the 36 stations in order to obtain mean climatology. The averaged pentad-mean data obtained by this procedure are in general still fluctuated, because the daily rainfall amount is a quite highly fluctuated quantity mainly due to atmospheric disturbances with time scales of a few days. To obtain smoothed seasonal variations, we apply a running average for every neighboring three pentads. The smoothed mean pentad data series (obtained by above-mentioned procedure at each station) is fit to an approximated formula defined by a sum of the annual (73-pentad) average, and two harmonics with periods of 73 (annual) and 36.5 (semi-annual) pentads by the least-square method. The approximation formula for a data series consisting of n points is given by:

$$y_t = \bar{y} + \sum_{k=1}^n \left\{ C_k \cos \left[\frac{2\pi kt}{n} - \varphi_k \right] \right\} \quad (1)$$

$$C_k = [A_k^2 + B_k^2]^{1/2} \quad (2)$$

$$A_k = \frac{2}{n} \sum_{t=1}^n y_t \cos \left(\frac{2\pi kt}{n} \right) \quad (3)$$

$$B_k = \frac{2}{n} \sum_{t=1}^n y_t \sin \left(\frac{2\pi kt}{n} \right) \quad (4)$$

$$\varphi_k = \begin{cases} \tan^{-1} (B_k/A_k), & A_k > 0 \\ \tan^{-1} (B_k/A_k) \pm \pi, \text{ or } 180^\circ, & A_k < 0 \\ \pi/2, \quad 90^\circ, & A_k = 0. \end{cases} \quad (5)$$

where k is the number of full cycles executed during the n time units, $y(t)$ is the value at time t , \bar{y} is the estimated temporal mean value, C is the amplitude and φ is the phase angle or phase shift. A detailed description of the method to obtain least-square estimates for the parameters of the annual and higher harmonics of climate variables is provided in Wilks (1995).

Two indices derived from the modeled seasonality modes series were used to determine whether a particular series was unimodal or bimodal. The ratio of semi-annual range to annual range (R_2/R_1) provides an objective index for measuring the degree of bimodal or unimodal behavior of rainfall at a given location. Following Makhov (1985) R_1 and R_2 are derived from smoothed annual cycle constructed by taking the sum of the annual and semi-annual harmonics of the climatological pentad mean series. The smoothed seasonal cycle is either unimodal (single maximum and minimum) or bimodal (double maximum and minimum). The annual range (R_1) is defined by the difference between the primary maximum and minimum; while the semi-annual range (R_2) is

Table 1. Location and altitude of stations used in the study.

Station	Latitude(deg)	Longitude(deg)	Altitude(m)
Arua	3.05	30.92	1280
Bukoba	-1.33	31.82	1143
Bushenyi	-0.57	30.17	1590
Dagoretti	-1.3	36.75	1798
Dar	-6.87	39.2	53
Dodoma	-6.17	35.77	1120
Entebbe	0.05	32.45	1183
Garissa	-0.47	39.63	128
Gulu	2.75	32.33	1106
Kabale	-1.25	29.98	1867
Kakamega	0.28	34.78	1555
Kasese	0.18	30.1	959
Kigoma	-4.88	29.63	999
Kitgum	3.28	32.88	937
Kisumu	-0.1	34.75	1146
Lamu	-2.27	40.83	9
Lodwar	3.12	35.62	566
Makindu	-2.28	37.83	1000
Malindi	-3.23	40.1	3
Mandera	3.93	41.87	230
Marsabit	2.3	37.9	1219
Masindi	1.68	31.72	1146
Mbarara	-0.6	30.68	1412
Mombasa	-4.03	39.62	57
Moyale	3.53	39.03	1113
Musoma	-1.5	33.8	1147
Mwanza	-2.47	32.92	1139
Namulonge	0.53	32.62	1150
Narok	-1.13	35.83	1890
Nyahururu	-0.03	36.35	2374
Soroti	1.72	33.62	1127
Tabora	-5.08	32.83	1182
Tanga	-5.08	39.07	39
Tororo	0.68	34.17	1226
Voi	-3.4	38.57	578
Wajir	1.75	40.07	244

defined by the difference between the secondary maximum and minimum of the smoothed annual cycle. The minimum ratio of zero implies unimodal variation while the maximum ratio of unity implies perfect bimodal variation (the two maxima or minima are equal). Figure 2 presents a demonstration of how R_1 and R_2 are derived based on modeled seasonality modes for Kisumu station in Kenya (0.1°N , 37.75°E).

The second index used is the difference in the fractional variance explained by the modes, V_1-V_2 . The fractional variance carried by each Fourier harmonic, V_i is given by:

$$V_i = \frac{C_i^2}{(2V_t)}, \quad i = 1, 2 \quad (6)$$

where C_i is the amplitude of the i th harmonic and V_t the total

variance of the annual cycle. The quantity V_1+V_2 represents the fractional variance carried by the smoothed annual cycle, while the difference, V_1-V_2 is used to qualitatively delineate unimodal/bimodal regime areas. V_1-V_2 is a parameter ranging from $+1$ for a purely unimodal distribution of perfect sine shape to -1 for a pure bimodal distribution. A value of V_1-V_2 near zero indicates either that neither distribution fits or that both distributions equally fit well.

We further classify the stations considered for the harmonic analysis based on the amplitudes of annual and semi-annual components. Stations are classified into types A, B and C depending upon whether the annual (C_1) or semi-annual (C_2) component has the larger amplitude or if there is no significance difference in their amplitudes, and also types I and II depending on whether the maximum rainfall of smoothed mean pentad amount appears during March – May and October – December or in a different season of the year.

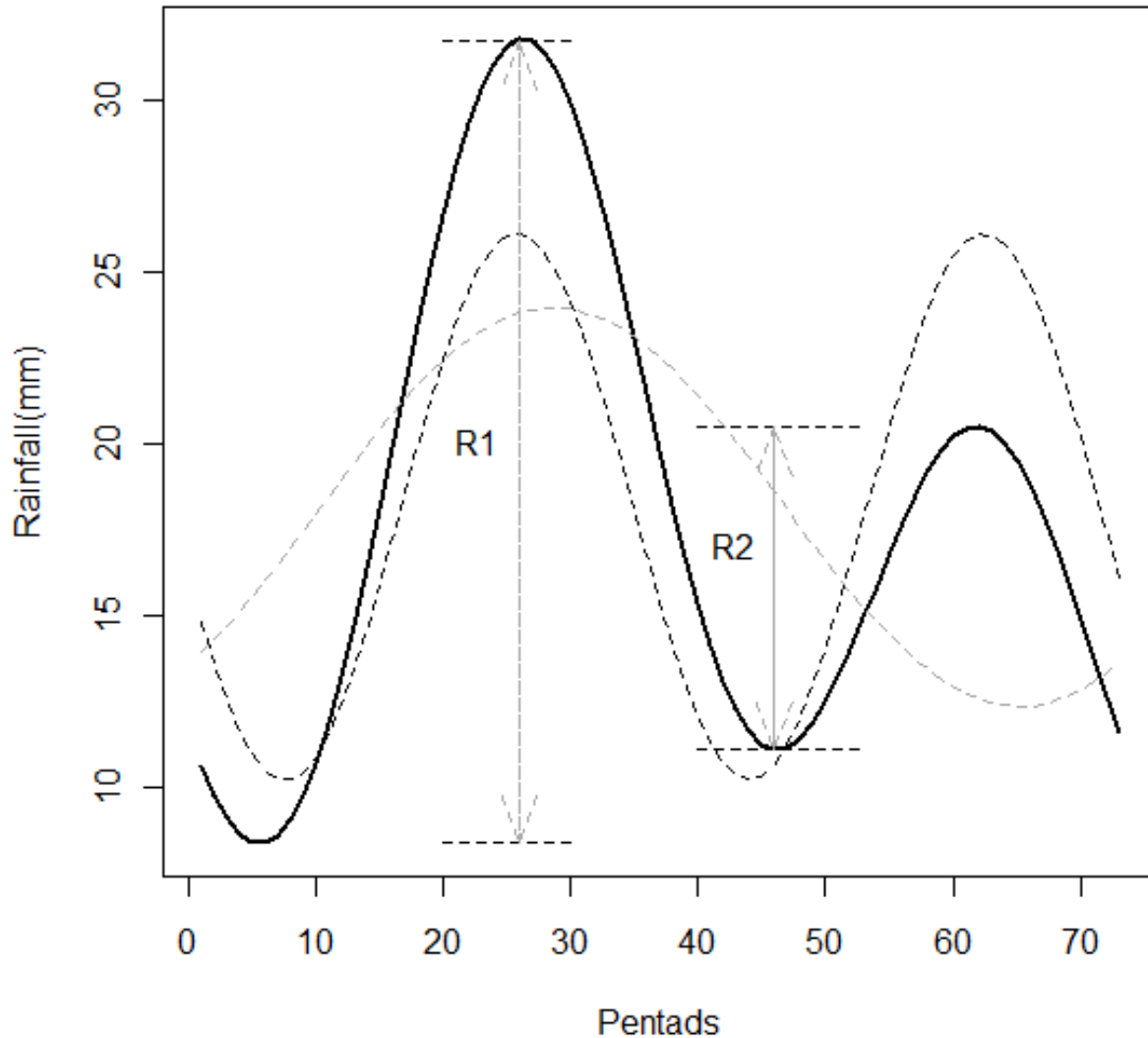


Figure 2: Bimodal seasonality of pentad mean rainfall (*solid black line*) and the corresponding components of the annual mean, annual (*grey dashed line*) and semi-annual (*black dashed line*) harmonics for Kisumu station in Kenya (0.1°N , 37.75°E). R_1 and R_2 indicate the annual range and apparent semi-annual range respectively.

RESULTS AND DISCUSSION

Distribution of Rainfall Seasonality Components

Table 2 provides a summary of the parameters used to measure the strength of the annual and semi-annual components of the seasonality of rainfall over East Africa at each station; while Figure 3 shows the spatial patterns of the two indices. Figure 3a displays the contours of the ratio of semi-annual to annual range (R_2/R_1) while Figure 3b shows the difference in fractional variance between the annual and semi-annual harmonics, $V_1 - V_2$. The pentad mean rainfall amount, annual and semi-annual components, and the derived mean annual cycle for some selected stations is also shown in Figure 4. Inspection of Table 2 and Figure 3 show that negative values of $V_1 - V_2$ depicting locations where bimodal rainfall

regime is stronger generally correspond well to R_2/R_1 exceeding 0.3 . This implies that a negative $V_1 - V_2$ indicates significant bimodal variation. In Figure 3a, the 0.3 contour is therefore used to demarcate the boundary between areas of unimodal and bimodal rainfall regimes. The figure reveals that the annual (73-pentad component) is dominant over Tanzania south of 3°S and west of 38°E . The profile of the annual cycle evolution in this part is depicted in Figure 4a for Tabora station with strong amplitude of the annual component ($C_1 = 15.9$) and weak semi-annual amplitude ($C_2 = 0.7$). For this station and others that fall within this area, the rainfall starts at around pentad 57 (8-12 October), reaches maximum in pentad 18 (27-31 March) and ends in the first week of May corresponding to pentad 25. Northern Uganda and the highland parts of Kenya are other regions where the annual component dominates.

Table 2. Indices used to delineate east African regions of unimodal and bimodal rainfall. C_1 and C_2 are the amplitude of the annual and semi-annual harmonics derived from equation (2), while V_1 and V_2 are fractional variances derived from equation (6). R_2/R_1 is the ratio of semi-annual range to annual range. The classification (CLASS) is based on the magnitude of the amplitudes of the first (C_1) and second (C_2) harmonics and seasons of peak rainfall (see explanation in the text)

STATION	C_1	C_2	CLASS	R_2/R_1	V_1	V_2	V_1-V_2
Arua	11.3	6.1	A-II	0.1	0.604	0.176	0.428
Bushenyi	5.9	7.3	B-I	0.4	0.313	0.481	-0.166
Entebbe	8.9	12.1	B-I	0.4	0.261	0.483	-0.221
Gulu	12.9	7.1	A-I	0.1	0.610	0.185	0.4258
Kabale	4	7.7	B-I	0.7	0.171	0.633	-0.462
Kasese	0.8	7.4	B-I	0.9	0.008	0.745	-0.736
Kitgum	13.8	5.2	A-II	0	0.719	0.102	0.617
Masindi	6.6	9.1	B-I	0.6	0.265	0.505	-0.239
Mbarara	3.9	7.6	B-I	0.5	0.161	0.614	-0.451
Namulonge	0.3	7.9	B-I	0.9	0.001	0.702	-0.701
Soroti	10.1	6.6	A-II	0.1	0.484	0.206	0.277
Bukoba	13.2	13.7	C	0.3	0.366	0.395	-0.028
Dar	10.6	11.8	B-I	0.3	0.302	0.374	-0.072
Dodoma	11.9	4	A-II	0.1	0.758	0.085	0.672
Kigoma	12.3	4.8	A-II	0.1	0.643	0.097	0.544
Moshi	12.8	11.1	C	0.2	0.344	0.258	0.085
Musoma	7.6	7.3	C	0.2	0.379	0.349	0.029
Mwanza	10.7	6.1	A-II	0.1	0.551	0.179	0.372
Tabora	15.9	0.7	A-II	0.1	0.824	0.001	0.823
Dagoretti	6.8	11.3	B-I	0.5	0.179	0.495	-0.316
Garissa	3.1	4.6	B-I	0.4	0.146	0.322	-0.175
Kakamega	9.7	7.1	A-I	0.2	0.479	0.257	0.223
Kisumu	5.7	7.8	B-I	0.4	0.225	0.421	-0.196
Lamu	13.2	12.6	C	0.2	0.377	0.344	0.033
Lodwar	1.5	1.6	B-I	0.3	0.167	0.189	-0.023
Makindu	7.8	6.9	A-I	0.2	0.322	0.252	0.069
Malindi	13.1	12.1	A-I	0.2	0.423	0.361	0.062
Mandera	1	5.5	B-I	0.8	0.018	0.569	-0.550
Maralal	4.4	0.7	A-II	0.1	0.496	0.012	0.484
Marsabit	4.8	9	A-I	0.5	0.121	0.426	-0.305
Mombasa	6.6	11.5	B-I	0.5	0.166	0.506	-0.339
Moyale	3.4	10.6	B-I	0.7	0.064	0.623	-0.558
Narok	7.1	2.9	A-II	0.1	0.623	0.104	0.519
Nyhururu	7.6	1.2	A-II	0.1	0.542	0.013	0.529
Voi	6.7	5.2	A-I	0.1	0.276	0.166	0.110
Wajir	2.1	4.5	B-I	0.6	0.104	0.478	-0.373

In northern Uganda, which receives rainfall for most of the year from early March with three peaks in May, August and October with light break in between, the annual component maximum is in pentad 47 (19-23 August). The second peak of rainfall in this region in August has been associated with the advection of moist air from Congo basin by mid-tropospheric westerlies (Okoola, 1999). For the highland parts of Kenya, that straddles the equator, the annual component peaks in July though the region receives peak rainfall in April,

followed by abrupt decrease between pentad 27 (11-15 May) to 32 (5-9 June), then an increase to September as depicted in Figure 4b for Nyahururu station which is 2374m above sea level. The area has a number of high mountains namely; Kenya (5895m), Elgon (4321m), Aberdare Ranges (3999m), and the Mau Escarpment (3098m). Also noteworthy is the high amplitude of the annual component ($C_1=7.6$) which is not comparable to the semi-annual component ($C_2=1.2$) despite the fact that this location is in the vicinity of the equator. The semi-

annual mode is more likely to be meaningful if it is at least comparable in magnitude to the annual mode in absolute sense (Chih-Ping and Wallace, 1976). It shows existence of two distinctive wet seasons where it is large compared to the annual cycle. The two seasons, namely March – May (MAM) and October – December (OND) coincide with the double passage of the ITCZ, which lags behind the overhead sun by 3-4 weeks over the region. They also coincide with the transition between the northeast and southeast monsoon circulations. The OND season is a transition period from the southeast monsoon to the northeast monsoon and vice versa for the MAM season. The transition period is associated with convergence along which the Inter-Tropical Convergence Zone (ITCZ) propagates. The ITCZ can be associated with a quasi-continuous belt of unsettled, often rainy weather (Folland et al. 1991). The convergence of these flows creates strong upward motion that causes rainfall if sufficient moisture is available. Even though the OND and MAM periods are considered transition periods, Nicholson (1996) described the air streams which govern the region's climate as the Congo air with westerly and southwesterly flow, northeast monsoon and the southeast monsoon. Both monsoons are thermally stable and associated with subsiding air. The Congo air is humid, convergent, and thermally unstable and generally associated with high amounts of rainfall. These air streams are separated by two surface convergent zones, the ITCZ and the Congo Air Boundary; the former separates the two monsoons, the latter, the easterlies and westerlies.

Normally, the passage of ITCZ leads the onset of the two rainy seasons by 3-4 weeks, but this may be modulated from season to season by the interactions between the ITCZ and perturbations in the global climate circulation, as well as with changes in the local circulation systems initiated by land surface heterogeneity induced by variable vegetation characteristics, large inland lakes and topography. The inter-annual variability of the East African climate is linked to perturbations in the global SSTs, especially over the equatorial Pacific and Indian Ocean basins, and to some extent, the Atlantic Ocean (Mutai and Ward, 2000; Indeje et al., 2000; Saji et al., 1999 among others). In particular, El Niño/Southern Oscillation (ENSO) anomaly patterns play a dominant influence on the interannual variability of the region. The zonal temperature gradient over the equatorial Indian Ocean, often referred to as Indian Ocean Dipole (IOD) Mode (Saji et al., 1999) and the coupled IOD-ENSO influence have also been linked to some of the wettest periods in the region, such as 1961, 1997 and 2006 (Black et al., 2003, Bowden and Semazzi, 2007; Owiti et al., 2008).

The parts of the region dominated by semi-annual component are indicated by contour lines of values greater than 0.3 in Figure 3a and negative contours in Figure 3b. Generally, the semi-annual components tend to be concentrated in two areas within the region. The

first is the region west of 35°E and lies between 2°N and 1.5°S equator which includes central and Southern Uganda, and the Lake Victoria regions of Kenya. Figure 4c provides the profiles of the annual and semi-annual components and the fitted annual cycle for Namulonge station from this area. This part of the region has a classical annual cycle of regions in the vicinity of equator, with two peaks in March-May and October – December coinciding with the passage of the ITCZ.

The second main area of semi-annual dominance is the eastern and northern and eastern Kenya, and the coastal areas of Kenya and Tanzania. The northern and eastern Kenya is semi-arid and generally receives less rainfall; this is indicated by the generally low amplitudes of the components in Figure 4d with rainfall confined only to the two seasons and almost zero rainfall during other months. The stations in northern Kenya basically receive seasonal rains only within the two months of April-May/October-November in the MAM/OND seasons. For the coastal areas depicted in Figure 4e, the dominant semi-annual peaks in MAM and OND seasons, with relatively dry periods in between. The double rainfall peak associated with the southeast and northeast monsoons trailing the twice overhead crossing of the sun. Figure 4f provides an example of the areas within the transition between annual and semi-annual dominant regions where the amplitude of the two components are almost equal though the semi-annual is evident in the smoothed pentad from the annual and semi-annual components. Stations under this category are characterized by values of $V_1 - V_2$ near zero indicating that neither of the modes dominates.

Due to under-sampling of stations over parts of the region especially southern and coastal Tanzania (Figure 3a), with only one station in the coastal Tanzania, there is uncertainty in the boundary between the two rainfall regimes defined by the two indices used due to spatial extrapolation between stations far apart. However, in the coastal strip of Tanzania in particular, climate is influenced by the Ocean via sea/ land circulations in most times of the year hence the unimodal regime signal is expected to be diffused. Analyses using more stations would however capture localized differences and probably provide a different picture. Inadequacy of gauge density over Africa including East Africa is provided in Parker et al. (2011). They noted that Mountainous areas (e.g. most of East Africa) and all zones on the edge of monsoon-penetration are likely to have highly intermittent, patchy rainfall so it is likely that >20 gauges will be needed per 2.5° grid box, and even more for 10-day rainfall which suffers greater, less coherent variations. These requirements are very rarely met in available data for Africa, so in general monthly gauge errors are likely to be much larger than 10%. So improvement of in situ data availability is important for achieving more representative results.

It is also noted that some seasonal changes shown in

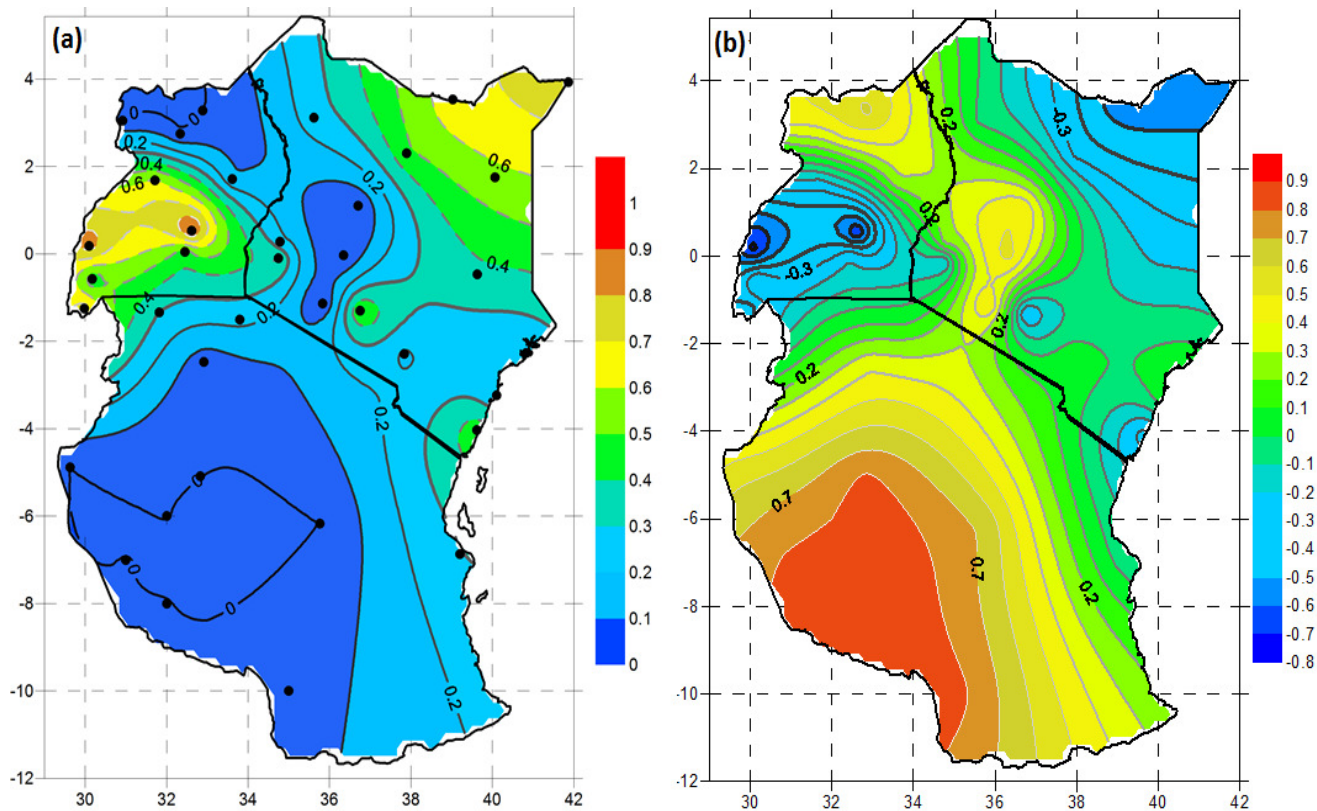
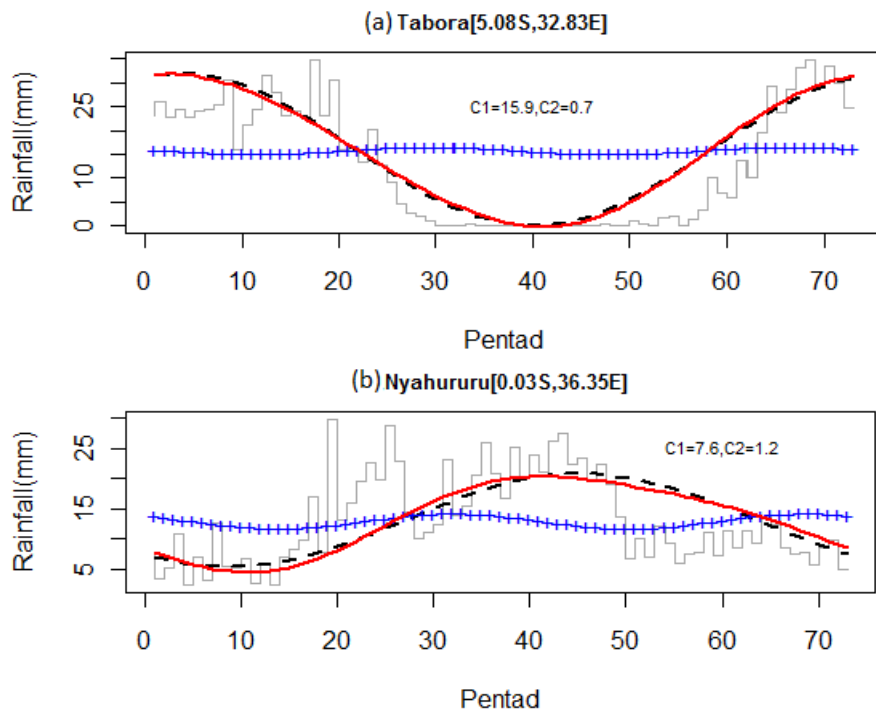


Figure 3: Contour plot of the ratio of (a) semi-annual to annual range, (R_2/R_1) and (b) the difference between fractional variance of annual (V_1) and semi-annual (V_2) harmonics, V_1-V_2 . In (a), the regions with unimodal ($R_2/R_1 < 0.3$) variations are indicated with thick contours while those with bimodal ($R_2/R_1 > 0.3$) are marked with dashed contours. In (b) positive values indicate unimodal regime and negative values indicate bimodal regime. Dots in (a) indicate the station locations.



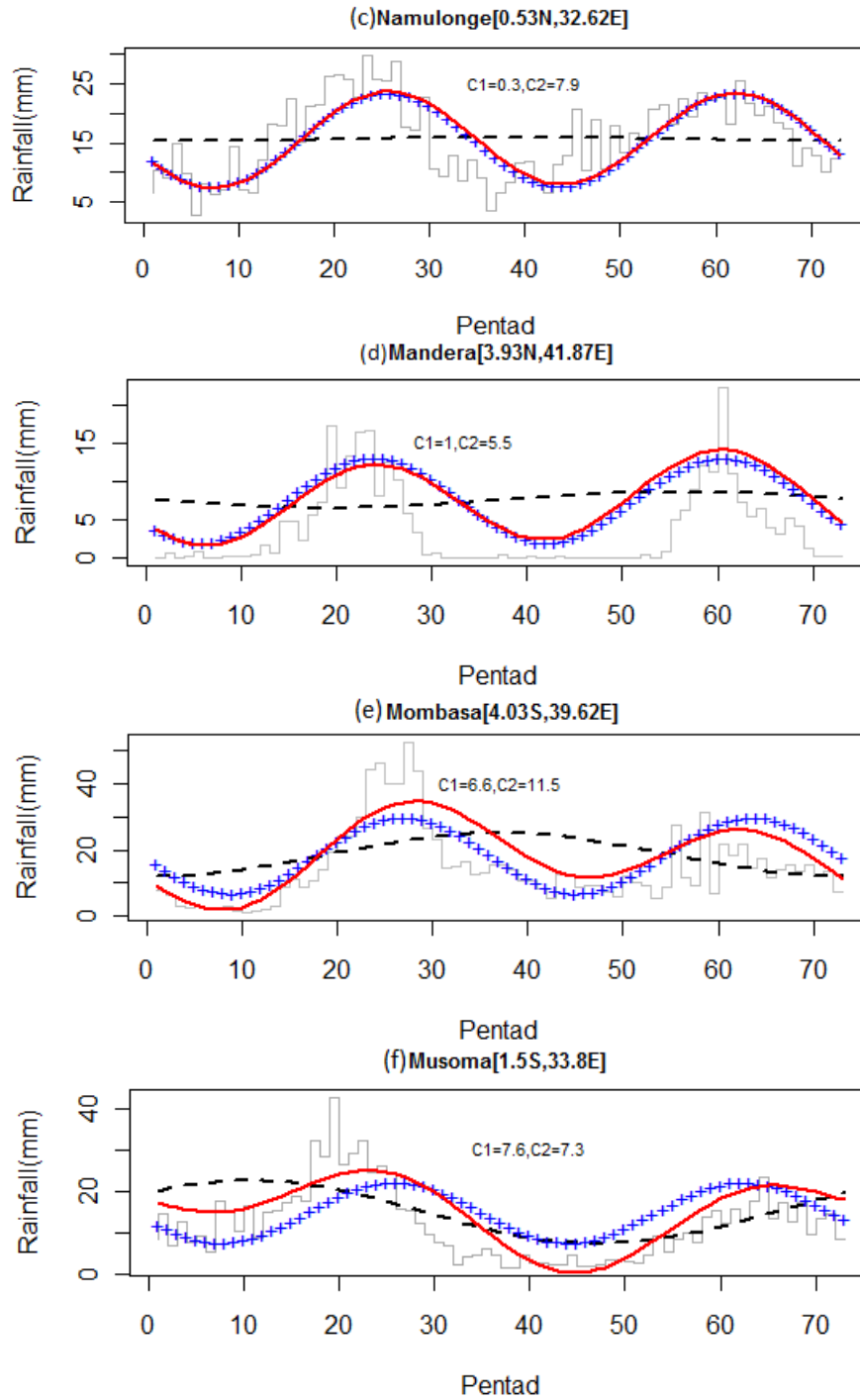


Figure 4: Pentad mean rainfall amount (dark grey step-bars) for selected stations. Dashed black and blue (+) curves show 73 pentad (annual) and 36.5 pentad (semi-annual) components respectively, which are fitted to the averaged seasonal variation (bars). The solid red curve shows the smoothed pentad rainfall variation, which is defined by the summation of the two components of 73 and 36.5 pentad periods. The amplitudes of annual (C_1) and semi-annual (C_2) components are also indicated in the figures.

Figure 4 are too sharp to be represented by the sine wave decomposed by Fourier transform. For example,

the annual cycle in Figure 4e can be interpreted as merely a computational mode. The Fourier Transform

(FFT) which uses basis functions that are sine and cosine functions, is designed to work with linear and stationary signals. The amplitudes and frequencies of each basis function are time-independent. Therefore, Fourier analysis is a global analysis, which can describe the frequency content of a signal and works well when the input signal is linear and stationary (Qian, 2002). Therefore, the method is unable to characterize processes that change frequency over time. Since the variations in climate variables are complex non-linear and non-stationary in nature, adaptive decomposition techniques like Empirical Mode Decomposition (Huang et al, 1998), which can decompose nonlinear and non-stationary signal time series into a definite number of components with different frequencies without any predetermined basis functions should be adopted in future studies.

Climatological Classification

A climatological classification was objectively obtained as long as a station had a clear seasonal variation, by using amplitudes and the ratio R_2/R_1 of the annual and semi-annual components, based on the harmonic analysis. The classification for each station is indicated in Table 2 such that A-I/B-I is a station where the annual/semi-annual mode dominates and the two maximum(s) are in MAM and/or OND. For stations with stronger annual/semi-annual component but with maximum neither in the two major seasons, the classification is A-II/B-II. The stations where neither of the two modes dominates with values of V_1-V_2 near zero were classified as C. Most of these stations for example Bukoba, Moshi and Musoma falls in areas of transition between annual and semi-annual regimes.

The results from analysis of the annual cycle components suggest that the seasonality of rainfall over the whole region does not follow the classical scheme of regular north-south transition of the peak rainfall with a time lag following the overhead sun. This scenario is only true for the western strip of the region (29°E to 34°E), where the annual component dominates areas that are north/south of 2° N/S of the equator while the semi-annual component dominate the areas within 2° north and south of the equator. On basis of this disparity, the region was also spatially delineated into 3 sub-regions based on the meridional characteristics of annual cycle components. Figure 5 provides a latitude-time cross section of zonally averaged mean rainfall over the three sub-regions to visualize aspects of rainfall seasonality from a time-latitude perspective. The University of Delaware $0.5^\circ \times 0.5^\circ$ gridded rainfall data was used in generating Figure 5. The first sub-region is the western strip spanning from latitude 29°E to 34°E , where the classical meridional annual cycle structure exist. Figure 5a provides a space time diagram of zonal averaged rainfall over this sub-region. It shows that the southern

part of this region, south of 3°S has its single peak from November to April. The first peak for the areas in the vicinity of the equator is March to May (the long rains season), with maximum rainfall slightly south of the equator (about 0.5°S). The second peak, which is lesser in amount, is in October – December (the short rains season). The northern part of this sub-region with dominant annual component confined to areas north of 2°N receives the peak rainfall during the boreal summer.

The second delineated sub-region is the central strip which is basically dominated by the annual component. This sub-region lies between 34°E to 37°E and is dominated by the east African highlands. The southern areas of this region south of 6°S have peak rainfall in November to April while the equatorial areas has their peak in March to May with a continuation of above 90mm of rainfall up to December (Figure 5b). The northern parts of this sub-region are semi-arid and generally receive less than 60mm of rainfall per month on average.

The third sub-region is the eastern strip which includes the semi-arid eastern plains of Kenya and the coastal strip of east Africa, where the seasonality is dominated by the semi-annual mode, except for the southern coast of Tanzania south of 6°S . Figure 5c, showing the zonal averaged mean rainfall over the sub-region depicts two major rainfall regimes. The first is the March – May long rains season and the second is the October – November season. For the equatorial and northern parts, the long rains peak is confined to the months of March – May, while in the southern parts south of 6°S , it seems to be a continuation from December of previous year. This region receives rainfall associated with the extreme southward location of the ITCZ and partly with moisture influx from the Indian Ocean during the months of January and February. Between the months of July to September the region is relatively dry with the exception of the coastal areas between 1°S to 6°S receiving at most 30 mm between June and August due to sea/land breeze circulation system. The two peaks in this sub-region coincide with the southeast/northeast monsoon regimes associated with the double passage of the ITCZ. The coastal Tanzania south of 6°S has a stronger unimodal mode while that of coastal Kenya has bimodal mode.

Conclusions

In this study, we have investigated the geographical variation of seasonality of rainfall over East Africa on the basis of pentad rainfall data at 36 stations during 1962-2006. The harmonic analysis technique was used to model the modes of rainfall seasonal cycle. The ratio of the modeled semi-annual range (R_2) to annual range (R_1) was used as an objective index to measure the degree of bimodal or unimodal behavior of rainfall at a given station. The difference of the fractional variance (V_1-V_2) carried by each of the modeled components was used to

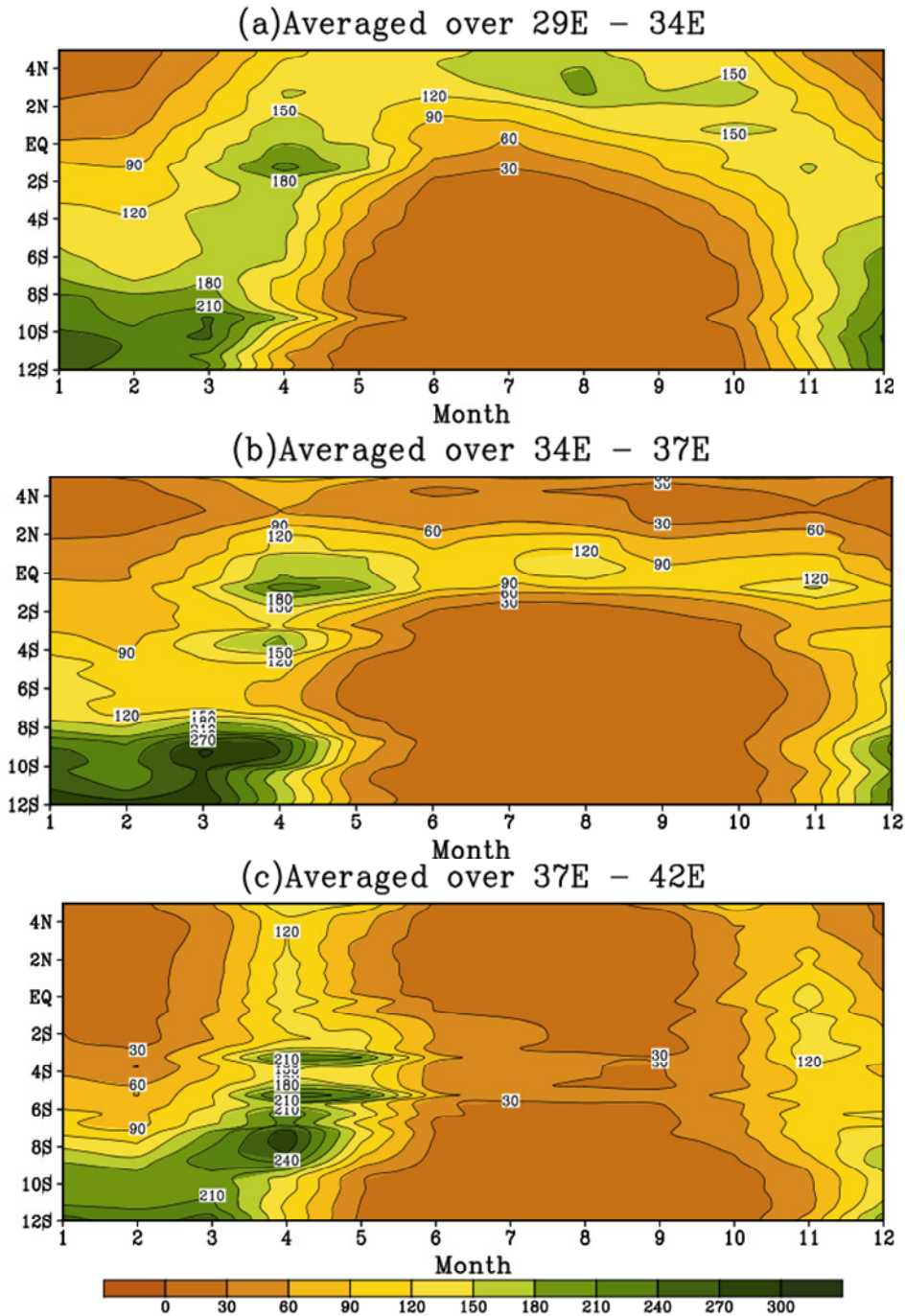


Figure 5: Time-latitude cross section of zonal averaged (1962-2006) monthly rainfall for (a) western (b) central and (c) eastern sub-regions of East Africa based on north-south structure of annual and semi-annual seasonality modes. The longitudes across which averaging was done are indicated on top of each figure.

qualitatively delineate areas of unimodal/bimodal regime. Stations were further classified based on the amplitude of the annual and semi-annual modes; and on whether the maximum rainfall of the smoothed annual cycle appears during MAM and OND seasons or in a different season of the year.

Results show that negative values of fractional variance difference, signifying bimodal regime, compares well to R_2/R_1 exceeding 0.3. The semi-annual mode is found to be dominant in central and southern Uganda; Lake Victoria region of Kenya; eastern and northern parts of Kenya; and coastal areas of Kenya and Tanzania. In

these areas, rainfall peaks in MAM and OND seasons except in northern Kenya, where the peaks are confined the months of April-May and October-November and hence are classified as B-I. The strongest signal of annual mode was found over Tanzania, south of 3°S and west of 38°E. The onset of rainfall in this area is in pentad 57(8-12 October) and reaches maximum in pentad 18(27-31 March). Northern Uganda also exhibits annual mode dominance with peak rainfall in pentad 47(19-23 August). These regions were classified as A-II. Though the highland areas of Kenya which straddles the equator may be expected to have semi-annual mode dominance, the results for some stations suggest that annual component is stronger. These are stations found in the highest areas of the central highland which are relatively wet throughout the year. However stations to the eastern highlands for example Dagoretti station in Nairobi exhibits bimodal rainfall regime. Thus we wish to note that if analysis based on a denser network of stations is done, the unimodal regime could be confined only to the central highlands.

Results from this study have further shown that the seasonality of rainfall over the whole region does not follow the classical scheme of regular north-south transition of the peak rainfall with a time lag following the overhead sun except for the western strip of the region (29°E to 34°E), where the annual component dominates areas that are north/south of 2° N/S of the equator while the semi-annual component dominate the areas within 2° north and south of the equator. This has been visualized by the latitude-time cross-section of the annual cycle for the three delineated zones based on 1962-2006 period using the high resolution gridded data.

Results obtained in this study provide a background for the next part of this study that will assess changes in seasonality of rainfall and boundaries between areas of common rainfall distribution over decadal periods; and validate predictions of seasonal patterns by climate models under present day and "greenhouse induced" climate change based on parameters used in this study.

Acknowledgements

The first author of this study is supported by the Chinese Scholarship Council (CSC) and the Government of Kenya through the National Council for Science and Technology (NCST).

REFERENCES

- Black E, Slingo J, Sperber KR (2003). An observational study of the relationship between excessively strong Short rains in coastal east Africa and Indian Ocean SST. *Mon. Weather. Rev.* 131:74-94.
- Bograd SF, Schwing F, Mendelssohn R, Green-Jessen P (2002). On the changing seasonality over the North Pacific. *Geophys. Res. Lett.* 29:9-12.
- Bowden J, Semazzi FHM (2007). Empirical analysis of intraseasonal climate variability over the Greater Horn of Africa. *J. Climate* 20(23):5715-5731.
- Camberlin P, Philippon N (2002). The East African March-May rainy season: Associated atmospheric dynamics and predictability over the 1968-97 period. *J. Climate* 15:1002-1019.
- Chih-Ping F, Wallace JM (1976). The Global Distribution of the Annual and Semiannual Cycles in Precipitation. *Mon. Wea. Rev.* 104:10930-1101.
- Filkenstein PL, Truppi LE (1991). Spatial distribution of rainfall seasonality in the United States. *J. Climate* 4:373-385.
- Folland CK, Owen JA, Ward MN, Colman AW (1991). Prediction of seasonal rainfall in the Sahel region of Africa using empirical and dynamical methods. *J. Forecasting* 10:2-56.
- Giannini A, Biasutti M, Held IM, Sobel AH (2008). A global perspective of African Climate. *Climatic Change* 90:359-383.
- Hamada JI, Yamanake MD, Masumoto J, Fukao S, Winarso PA, Sribimawati T (2002). Spatial and temporal variations of the rainy season over Indonesia and their link to ENSO. *J. Meteor. Soc. Jpn.* 80:285-310.
- Hastenrath S, Polzin D, Mutai CC (2007). Diagnosing the 2005 Drought in equatorial East Africa. *J. Climate* 20:4628-4637.
- Huang NE, Shen Z, Long SR, Wu MC, Shih HH, Zheng Q, Yen N, Tung CC, Liu HH (1998). The empirical mode decomposition method and the Hilbert spectrum for non-stationary time series analysis. *Proc. Roy. Soc. London*, 454A:903-995.
- Indeje M, Semazzi FHM, Ogallo LJ (2000). ENSO signals in East African rainfall and their prediction potentials. *Int. J. Climatol.* 20:19-46.
- Latif M, Dommengot D, Dima M (1999). The role of Indian Ocean sea surface temperature in forcing east African climate anomalies during winter 1998. *J. Climate* 12:3479-3504.
- Makhov LL (1985). Method of Amplitude-Phase characteristics for analyzing climate dynamics. *Meteor. Gidrol.* 5:80-89.
- Mpeta EJ, Jury MR (2005). The annual cycle of African climate and its variability. *Water SA.* 31(1):1-8.
- Mutai CC, Ward MN (2000). East African rainfall and the tropical circulation/convection on intra-seasonal to interannual timescales. *J. Climate* 13:3915-3939.
- Nicholson SE (1996). A review of climate dynamics and climate variability in eastern Africa. In: Johnson TC, Odada E (eds). *The Limnology, Climatology and Paleoclimatology of the East Africa Lakes*, Gordon and Breach, Amsterdam pp.25-56.
- Nicholson SE (2001). A semi-quantitative regional data set for studying African climate of the nineteenth century, Part 1. Overview of the data set. *Climatic Change* 50:317-353.
- Okoola RE (1999). A diagnostic study of the East African monsoon circulation during the northern hemisphere spring season. *Int. J. Climatol.* 19:143-169.
- Owiti ZO, Ogallo LA, Mutemi J (2008). Linkages between the Indian Ocean Dipole and east African seasonal rainfall anomalies. *J. Kenya Meteor. Soc.* 2:3-17.
- Parker D, Good E, Chadwick R (2011). Reviews of observational data availability over Africa, for monitoring, attribution and forecast evaluation. Met Office, Hadley Center Technical Note 86.
- Pezzulli S, Stephenson DB, Hannachi A (2005). The variability of seasonality. *J. Climate* 18:71-88.
- Qian S (2002). *Introduction to Time-Frequency and Wavelet Transforms*. Prentice-Hall Inc Upper Saddle River, NJ.
- Saji NH, Goswami BN, Vinayachandran PN, Yamagata T (1999). A dipole mode in the tropical Indian Ocean. *Nature* 401:360-363.
- Shen SP, Shu T, Huang NE, Wu Z, North GR, Carl TR, Easterling DR (2005). HHT analysis of the nonlinear and non-stationary annual cycle of daily surface air temperature data. In: Huang NE, Shen SSP (eds). *Hilbert-Huang transform: introduction and applications*. World Scientific, Singapore pp.187-210.
- Shongwe ME, van Oldenborgh, van Aalst (2011). Projected changes in mean and extreme precipitation in Africa under global warming, Part II: East Africa. *J. Climate* 24:3718-3731.
- Thompson R (1999). A time-series analysis of the changing seasonality of precipitation in the British Isles and neighbouring areas. *J. Hydrol.* 224:169-183.
- Webster PJ, Moore AM, Loschigg JP, Leben RR (1999). Coupled

- ocean-atmosphere dynamics in the Indian Ocean during 1997/98. *Nature* 401:356-360.
- Whitfield PH, Bodtker K, Cannon AJ (2002). Recent variations in temperature and precipitation in Canada. *Int. J. Climatol.* 22:1617-1644.
- Wilks D (1995). *Statistical Methods in Atmospheric Sciences*. Academic Press, New York pp.325-341.
- Willmott CJ, Matsuura K. (2009). A revised 100-year plus gridded time series of monthly precipitation and air temperature for the global land surface: Monthly time series (1900–2008) Version 2.01. [Available online at <http://climate.geog.UDEL.edu/climate/>]. Website accessed 25 November, 2010.
- Wu Z, Schneider EK, Kirtman BP, Sarachik ES, Huang NE, Tucker CJ (2008). Amplitude-frequency modulated annual cycle: an alternative reference frame for climate anomaly. *Climate Dynamics*. DOI 10.1007/s00382-008-0437-z.